Flotillin microdomains interact with the cortical cytoskeleton to control uropod formation and neutrophil recruitment

Alexander Ludwig,[1] Grant P. Otto,[1] Kirsi Riento,[1] Emily Hams,[2] Padraic G. Fallon,[2] and Ben J. Nichols[1]

[1]MRC Laboratory of Molecular Biology, Cambridge CB2 0QH, England, UK
[2]Institute of Molecular Medicine, Trinity College Dublin, Dublin 2, Ireland

We studied the function of plasma membrane microdomains defined by the proteins flotillin 1 and flotillin 2 in uropod formation and neutrophil chemotaxis. Flotillins become concentrated in the uropod of neutrophils after exposure to chemoattractants such as N-formyl-Met-Leu-Phe (fMLP). Here, we show that mice lacking flotillin 1 do not have flotillin microdomains, and that recruitment of neutrophils toward fMLP in vivo is reduced in these mice. Ex vivo, migration of neutrophils through a resistive matrix is reduced in the absence of flotillin microdomains, but the machinery required for sensing chemoattractant functions normally. Flotillin microdomains specifically associate with myosin IIa, and spectrins. Both uropod formation and myosin IIa activity are compromised in *flotillin 1* knockout neutrophils. We conclude that the association between flotillin microdomains and cortical cytoskeleton has important functions during neutrophil migration, in uropod formation, and in the regulation of myosin IIa.

Introduction

Microdomains defined by the proteins flotillin 1 and flotillin 2 (also termed reggie 2 and reggie 1, respectively) are an apparently ubiquitous feature of mammalian cells (Babuke and Tikkanen, 2007). They reside in the plasma membrane, as well as in endosomal and lysosomal organelles (Bickel et al., 1997; Lang et al., 1998; Volonte et al., 1999). The precise molecular function of flotillin microdomains is not known, but they are thought to be involved in processes including insulin signaling, T cell activation, phagocytosis, epidermal growth factor signaling, and regrowth of neurons (Babuke and Tikkanen, 2007; Langhorst et al., 2007; Hansen and Nichols, 2009). Non-exclusive models for how the microdomains act during these processes include mediation of endocytosis, scaffolding of signaling proteins, and interaction with the cortical cytoskeleton (Glebov et al., 2006; Kato et al., 2006; Babuke and Tikkanen, 2007; Langhorst et al., 2007).

Recently, it was shown that flotillin microdomains accumulate rapidly in the uropod of neutrophils after stimulation with the chemotactic bacterial peptide N-formyl-methionyl-leucyl-phenylalanine (fMLP; Rajendran et al., 2009; Rossy et al., 2009). The uropod is a plasma membrane protrusion found at the rear of motile leukocytes and other cell types (Sánchez-Madrid and Serrador, 2009). Generation of this structure requires segregation of different types of protein and lipid plasma membrane components, and local recruitment and activation of components of the cortical cytoskeleton (Gómez-Mouton et al., 2001; Seveau et al., 2001; Xu et al., 2003; Lee et al., 2004). The uropod of migrating leukocytes has been implicated in several functions, including intercellular signaling, regulation of cell adhesion, and migration through resistive environments. Whether flotillin microdomains are required for uropod morphogenesis and function has yet to be directly tested in loss-of-function experiments.

Here we use a combination of biochemistry, imaging, and generation of *flotillin 1* knockout ($^{-/-}$) mice to investigate the function of flotillin microdomains in neutrophils.

The Rockefeller University Press $30.00
J. Cell Biol. Vol. 191 No. 4   771–781
www.jcb.org/cgi/doi/10.1083/jcb.201005140

JCB   771

Results and discussion

Flotillin 1⁻/⁻ mice lack flotillin microdomains

We produced C57BL6/J mice lacking exons 3–8 of the gene for flotillin 1 (Fig. 1, a and b). Western blots of tissues that express flotillin 1 in wild-type mice confirmed that flotillin 1 protein cannot be detected in *flotillin 1⁻/⁻* mice (Fig. 1 c). Heterozygous *flotillin 1⁺/⁻* mice had reduced levels of flotillin 1 protein compared with controls. *Flotillin 1⁻/⁻* mice are viable, fertile, and have no readily apparent phenotypes.

Flotillin 1 and flotillin 2 function together to generate flotillin microdomains, and reduction in the expression of one flotillin protein causes a reduction in the expression of the other (Frick et al., 2007; Langhorst et al., 2008; Babuke et al., 2009). Western blotting of tissues from *flotillin 1⁻/⁻* mice confirmed that in the absence of flotillin 1 the expression of flotillin 2 is greatly reduced (Fig. 1 c). Mouse embryonic fibroblasts (MEFs) grown from *flotillin 1⁻/⁻* and isogenic control mice were fixed and stained with antibodies against flotillin 1 and flotillin 2. In the controls, flotillin 1 and flotillin 2 colocalized in plasma membrane puncta as predicted. In the *flotillin 1⁻/⁻* cells the limited, weak staining obtained with flotillin 2 antibodies was uniformly distributed across the plasma membrane (Fig. 1 d). Intact flotillin microdomains are insoluble in cold nonionic detergents (Bickel et al., 1997). Solubilization of extracts from *flotillin 1⁻/⁻* and wild-type control MEFs with cold Triton X-100 followed by ultracentrifugation in a sucrose density gradient revealed that the residual flotillin 2 found in these extracts is not present in the detergent-resistant fraction (Fig. 1 e). These observations show that deletion of *flotillin 1* is likely to completely abrogate the function of flotillin microdomains.

Flotillin microdomains are required for neutrophil recruitment in vivo

We measured recruitment of neutrophils in vivo, using a cell recruitment model in which a sterile air pouch is introduced subcutaneously. This establishes a vascularized cavity that is ideal for monitoring cellular migration in response to chemotactic agents (Kadl et al., 2009). After injection of fMLP, the air pouch was lavaged at different time points, and cellular infiltration was assessed. Total cell counts were performed, and cytospin slides were prepared and stained with Wright-Giemsa. Reduced total numbers of cells accumulated in the air pouch in response to fMLP in *flotillin 1⁻/⁻* mice, relative to wild type (Fig. 2 a). Counting of the infiltrating cells on Giemsa-stained cytospins demonstrated that the reduced recruitment of cells into the air pouch of *flotillin 1⁻/⁻* mice was due to an early defect in neutrophil, monocyte, and lymphocyte recruitment, with the effect being most prominent in the case of neutrophils (Fig. 2, a and c).

To further confirm that fMLP-induced recruitment of neutrophils and monocytes is impaired in *flotillin 1⁻/⁻* mice, cells infiltrating the air pouch were characterized by flow cytometry (Fig. 2 b). Surface expression of Ly6G and CD11b, as well as forward/side scatter profiles, were used to identify neutrophils (Ly6G^hiCD11b^+ve) and monocytes (Ly6G^loCD11b^+ve; Cooper et al., 1993; Taylor et al., 2002). Monocytes were confirmed by F4/80 expression (not depicted). We detected a striking decrease

in neutrophil recruitment in *flotillin 1⁻/⁻* mice, with only 20% of control levels observed after 2 h (Fig. 2, b and c). We also detected fewer monocytes (P = 0.01) in the *flotillin 1⁻/⁻* mice (Fig. 2 c).

The basal populations of different cell types in the air pouch model before addition of fMLP were essentially the same in control and *flotillin 1⁻/⁻* mice (Fig. 2, a–c; zero time points). Hematological analysis of blood obtained by cardiac puncture from control and *flotillin 1⁻/⁻* mice showed that levels of circulating leukocytes are again the same in both cases (Fig. S1). The pronounced defect in the chemotaxis of *flotillin 1⁻/⁻* neutrophils into fMLP-containing skin pouches is, therefore, likely to be due to a role for flotillin microdomains specifically in the process of recruitment itself.

Flotillin microdomains interact with myosin IIa and spectrins

To gain insight into the molecular mechanisms underpinning the function of flotillin microdomains we immunoisolated flotillin microdomains, using anti-GFP antibodies and a HeLa cell line stably expressing flotillin 2–GFP. A second cell line expressing GFP provided a negative control. Elution of the immunoisolates was performed in a three-step protocol, to consecutively isolate detergent-resistant regions of the plasma membrane containing flotillin microdomains (E2), then specific protein complexes containing the microdomains themselves (E3; Fig. 3 a). After Coomassie staining, protein bands that were not present in the negative control samples were identified by mass spectrometry (Fig. 3 b). The most abundant proteins found in E3 were flotillins 1 and 2, indicating that the immunoisolation protocol works efficiently. Other abundant proteins found specifically associated with flotillin microdomains were α- and β-spectrins and myosin heavy chain 9, the heavy chain of myosin IIa (Conti and Adelstein, 2008; Vicente-Manzanares et al., 2009; Fig. 3 b).

Western blotting was used to confirm the specific association of α-spectrin and myosin IIa with flotillin microdomains, using the same sequential elution procedure. As predicted, both proteins were found enriched in the E3 fraction after immunoisolation of flotillin 2–GFP from HeLa cells (Fig. 3 c). Caveolin 1 was not found to be directly associated with flotillin microdomains. Only trace amounts of actin were detected in the flotillin microdomain (E3) fraction, and abundant plasma membrane proteins including cadherins, syntaxin 2, and the transferrin receptor were not detected (Fig. 3 c). We conclude that flotillin microdomains are specifically associated with myosin IIa and both α- and β-spectrins.

Flotillin microdomains may represent a point of contact between the plasma membrane and the underlying cell cortex. To support this idea, we coexpressed flotillin 1–GFP, flotillin 2–GFP, and myosin IIa–mCherry in HeLa cells. As myosin IIa is found throughout the cell cortex, the significance of colocalization between flotillin microdomains and myosin IIa is hard to assess. We therefore disrupted the cell cortex using cytochalasin D. This causes rapid lateral retraction of myosin IIa–mCherry from large regions of the base of the cell. TIR (total internal reflection) imaging revealed lateral movement of flotillin microdomains within the plane of the plasma membrane that was completely coincident with this retraction of myosin IIa–mCherry
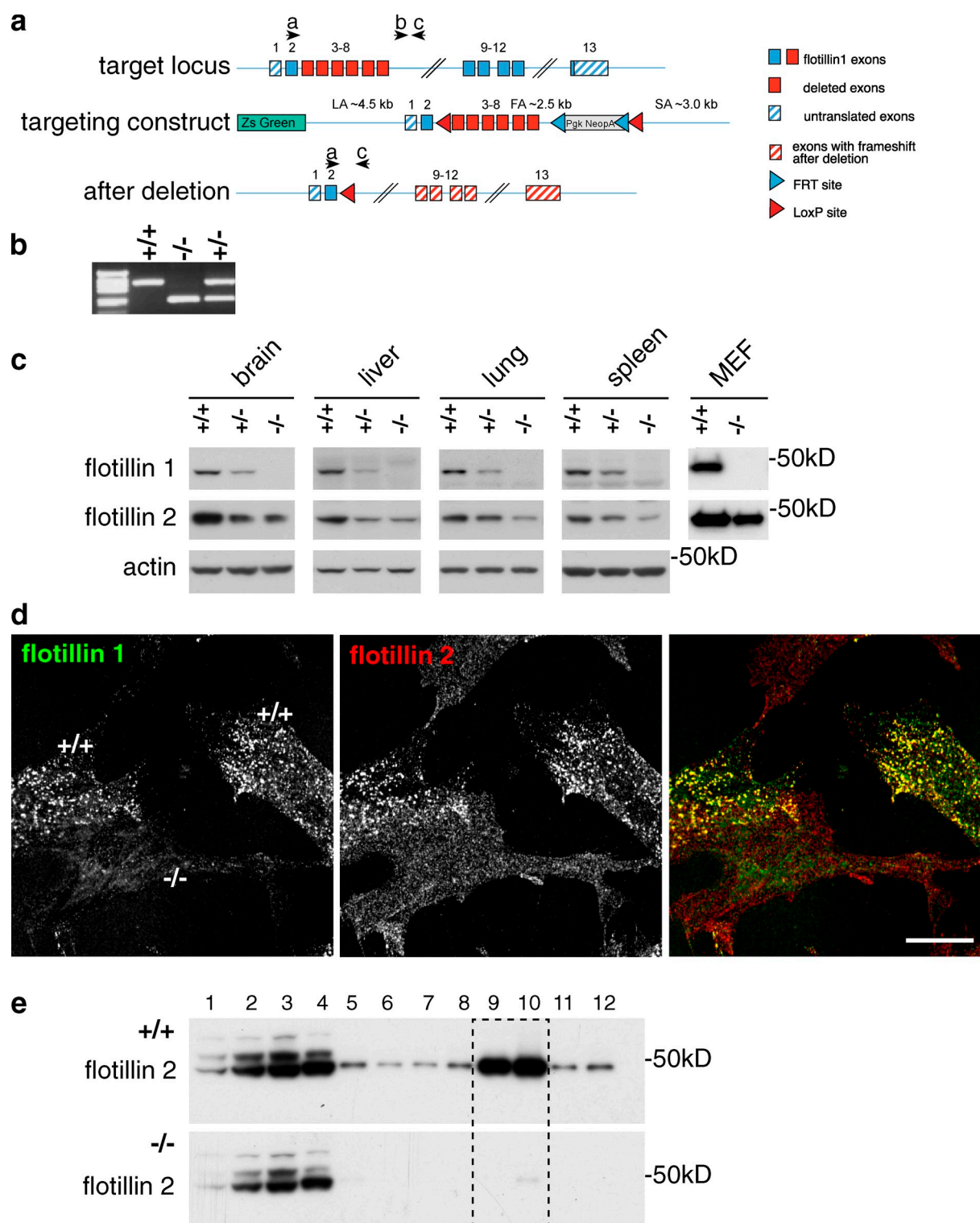
Figure 1. **Flotillin microdomains are absent in *flotillin 1*⁻/⁻ mice.** (a) Gene targeting strategy. Positions of primers used for PCR genotyping are shown as black arrows; the primers are labeled a, b, c. (b) Genotyping of wild-type, C57Bl6/J *flotillin 1*⁺/⁺ (+/+), flotillin 1 knockout C57Bl6/J *flotillin 1*⁻/⁻ (−/−), and *flotillin 1*⁺/⁻ heterozygous mice (+/−). (c) *Flotillin 1*⁻/⁻ mice lack flotillin 1, and flotillin 2 expression in these mice is drastically reduced. Western blots using antibodies against flotillin 1 and flotillin 2. MEF, mouse embryonic fibroblast. (d) Residual flotillin 2 in *flotillin 1*⁻/⁻ MEFs is not concentrated in flotillin microdomains. Staining of mixed culture of *flotillin 1*⁻/⁻ and wild-type MEFs with flotillin 1 and flotillin 2 antibodies. Bar, 20 µm. (e) Residual flotillin 2 in *flotillin 1*⁻/⁻ MEFs is not present in detergent-resistant membranes. Detergent-resistant membranes (fractions 9 and 10, boxed) were floated in a sucrose density gradient. Western blots of samples from control (+/+) and *flotillin 1*⁻/⁻ (−/−) mice were probed with antibodies to flotillin 2.

Figure 2. **Neutrophil migration requires flotillin microdomains.** (a) fMLP (1 µg/mouse) was injected into subcutaneous air pouches. At the times indicated, mice were culled and the air pouch lavaged with PBS. Leukocyte counts were performed based on cell morphology after staining with Wright-Giemsa; a total of 200 cells were counted per slide. +/+, wild type; −/−, flotillin 1 knockout. Results are mean ± SEM (n = 3–7); these data are representative of three individual experiments. *, P < 0.05. (b) Cellular infiltration of the air pouch was monitored by flow cytometry using CD11b and Ly6G expression as markers of neutrophils (Ly6G^{hi}CD11b^{+ve}) and monocytes (Ly6G^{lo}CD11b^{+ve}), as shown by the blue gating regions. Numbers in blue are the percentages of total cells in each gate. (c) Absolute cell numbers calculated from FACS analysis of infiltrating cells as in panel b. Results are mean ± SEM (n = 3–7); data are representative of three individual experiments. *, P < 0.05.
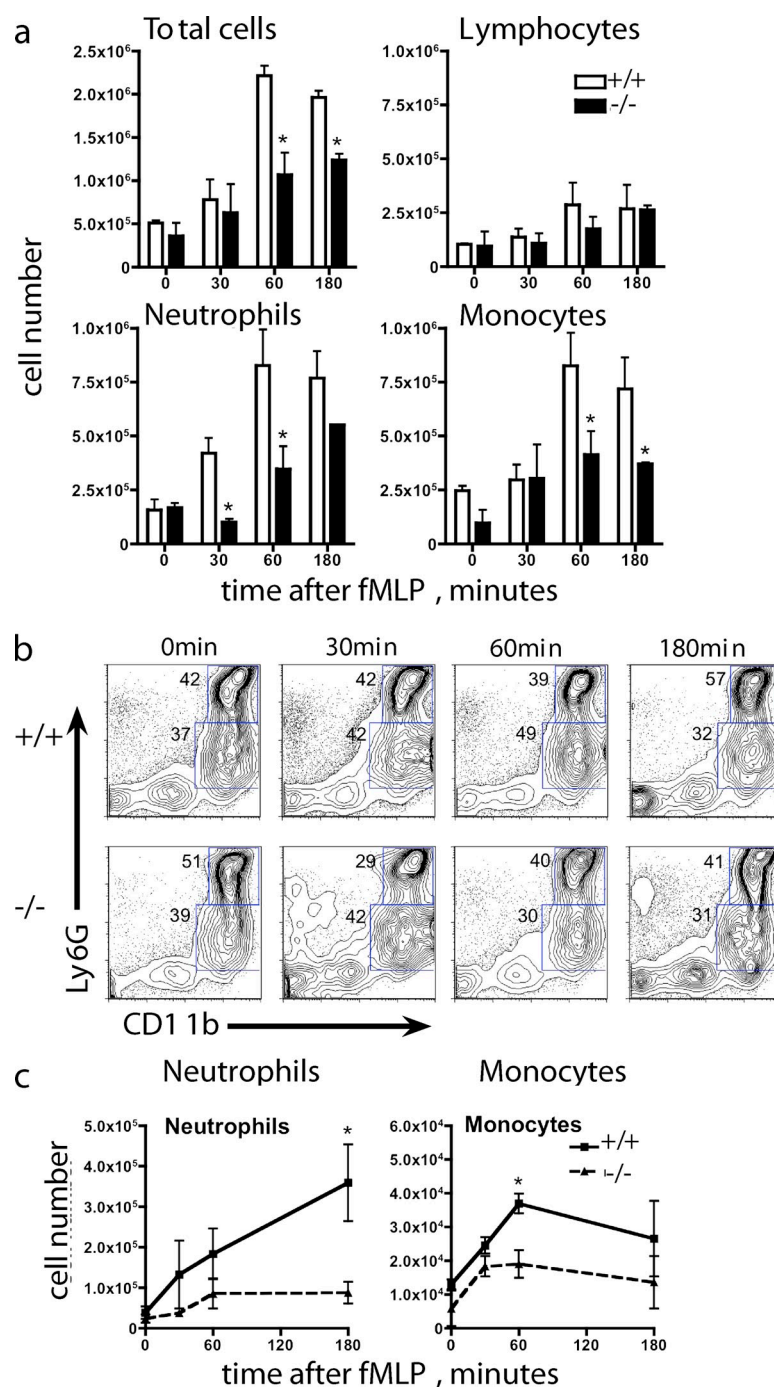
(Fig. 4 a, and Video 1). This provides direct evidence that flotillin microdomains are associated with the cell cortex in live cells.

We next performed experiments designed to assess whether flotillin microdomains can impact on the activity of myosin IIa. Phosphorylation of myosin IIa regulatory light chain (RLC) at Ser19 increases motor activity and plays a key role in the regulation of its cellular activity (Umemoto et al., 1989; Conti and Adelstein, 2008). Overexpressing flotillins, particularly flotillin 2, induces changes in cell morphology, and hence presumably in the distribution or activity of cortical proteins (Neumann-Giesen et al., 2004, 2007; Hoehne et al., 2005). We generated individual HeLa cell lines stably overexpressing

flotillin 2–GFP. Staining of flotillin 2–GFP cells with anti-flotillin 1 antibodies showed that flotillin 1 expression is increased in these cells (Fig. S2). This suggests that exogenously expressed flotillin 2–GFP stabilizes endogenous flotillin 1. Flotillin 2–GFP cells frequently had altered morphology compared with untransfected controls, and the distribution (but not total expression) of myosin IIa was visibly altered (Fig. 4 b). The expression and distribution of α- or β-spectrin was not notably altered in these cells (not depicted). Staining of the flotillin 2–GFP cell lines with phosphospecific antibodies revealed a pronounced increase in myosin IIa RLC phosphorylation as compared with cocultured control HeLa cells (Fig. 4, c and d). Increased myosin IIa
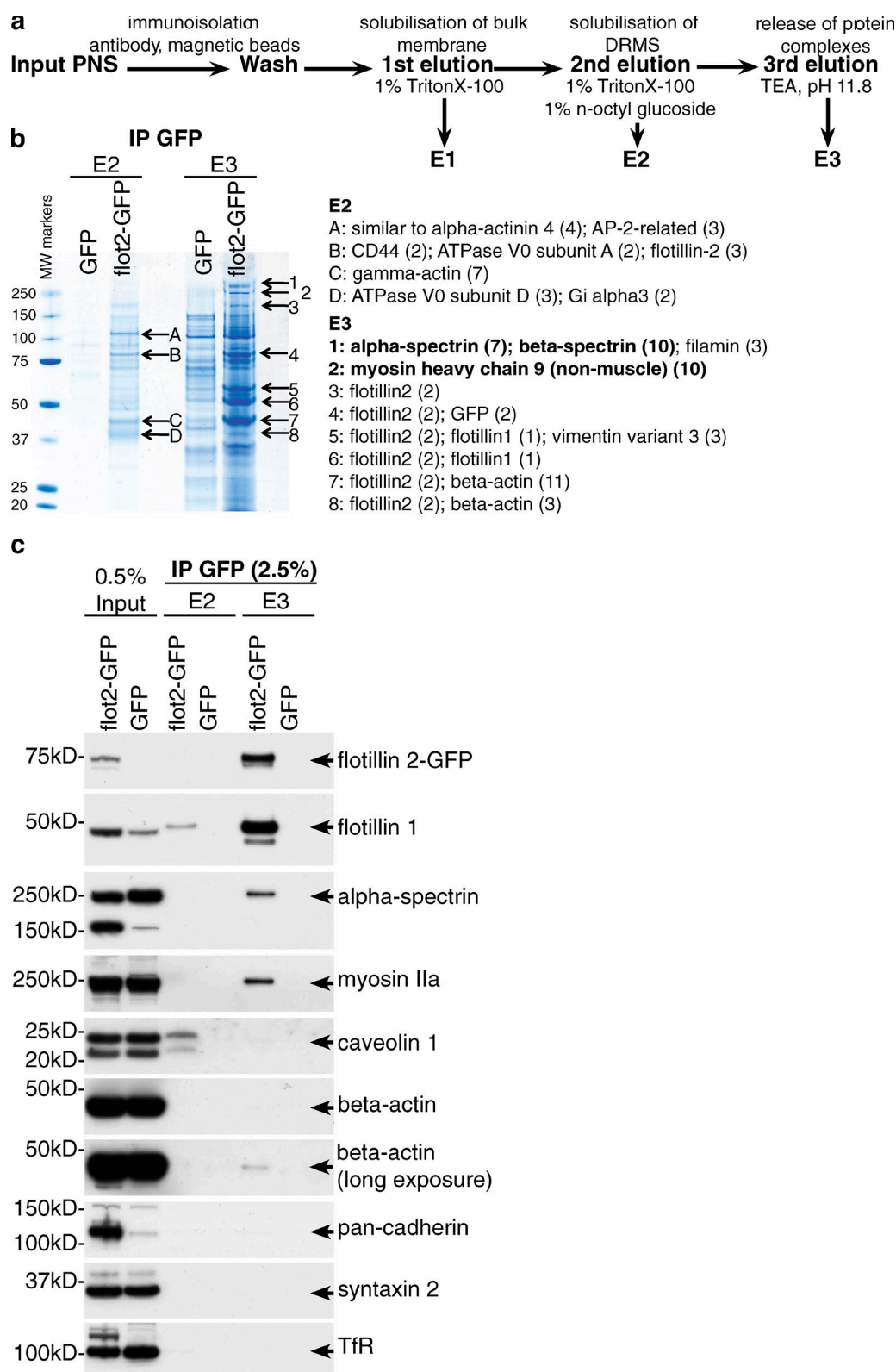
Figure 3. **Flotillin microdomains associate with myosin IIa and spectrins.** (a) Protocol for isolation of flotillin microdomains. (b) Identification of proteins associated with flotillin microdomains in HeLa cells by mass spectrometry. The specific bands from Coomassie-stained gels indicated with arrows were identified by mass spectrometry. Numbers in brackets indicate the number of unique peptides identified. MW, molecular weight (kD). (c) Confirmation that α-spectrin and myosin IIa associate specifically with flotillin microdomains in HeLa cells. Immunoisolation was performed as in panels a and b above; samples were analyzed by Western blotting with antibodies against the proteins indicated.
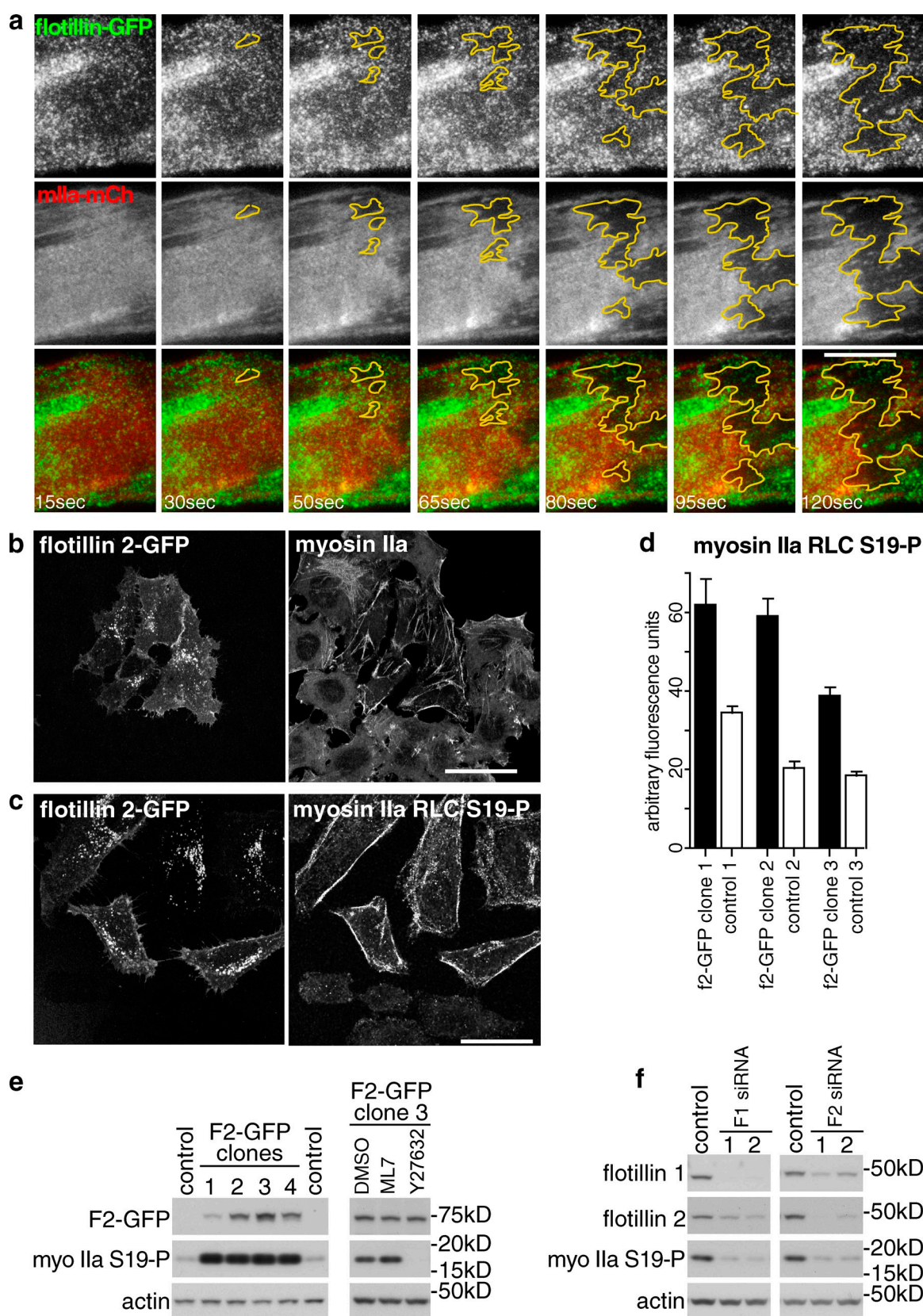
Figure 4. **Flotillin microdomains interact with the cell cortex in vivo, and regulate myosin IIa activity.** (a) Co-migration of flotillin microdomains and myosin IIa. Time-lapse TIR imaging of a HeLa cell coexpressing flotillin–GFP and myosin IIa–mCherry. Times indicate interval after addition of 50 µM cytochalasin D. The yellow area highlights the region of the plasma membrane from which both flotillin microdomains and cortical cytoskeleton retract. Bar, 10 µm. (b) Stable overexpression of flotillin 2–GFP alters the distribution of myosin IIa. A HeLa cell line overexpressing flotillin 2–GFP was co-cultured with HeLa cells, and stained with antibodies against the heavy chain of myosin IIa. Bar, 25 µm. (c) Stable overexpression of flotillin 2–GFP increases phosphorylation

RLC phosphorylation in the flotillin 2–GFP cell lines was confirmed by Western blotting (Fig. 4 e). Use of the myosin light chain kinase inhibitor ML7 (Chou et al., 2004), and the Rho kinase inhibitor Y27632 (Saito et al., 2002), confirmed the specificity of the antibodies and identified Rho kinase as being responsible for the bulk of the detected phosphorylation (Fig. 4 e). We used siRNAs to look at the effect of reduced flotillin 1 or flotillin 2 expression on phosphorylation of myosin IIa RLC in HeLa cells. Two separate siRNAs against each flotillin all caused a clear reduction in myosin IIa RLC phosphorylation (Fig. 4 f). Therefore, an increase in the abundance of flotillins is sufficient to increase the activity of myosin IIa, and loss of flotillins causes a reduction in activity.

Uropod formation and cell migration is compromised in the absence of flotillin microdomains

We sought to apply the data derived from experiments in HeLa cells described above to begin to characterize the functional deficit in neutrophils from *flotillin 1*$^{-/-}$ mice in more detail. Both spectrins and myosin IIa, like flotillin microdomains, are found concentrated in uropods (Gregorio et al., 1992; Eddy et al., 2000; Jacobelli et al., 2009; Sánchez-Madrid and Serrador, 2009) and myosin IIa activity is required for uropod formation (Doyle et al., 2009; Jacobelli et al., 2009; Vicente-Manzanares et al., 2009). We asked, therefore, whether the absence of flotillin microdomains impacts on neutrophil migration ex vivo, uropod formation, or myosin IIa activity.

Chemotaxis assays following the migration of neutrophils from control and *flotillin 1*$^{-/-}$ mice on serum-coated glass in a concentration gradient of fMLP, using Dunn chambers and video microscopy, did not detect any difference between the two populations of cells (Fig. S3, a and b). Additionally, phosphorylation of ERK (extracellular signal–regulated kinase), which acts downstream of the fMLP receptor (Coxon et al., 2003), occurs identically in control and *flotillin 1*$^{-/-}$ cells (Fig. S3, c and d). We also tested the ability of control and *flotillin 1*$^{-/-}$ neutrophils to migrate in Dunn chambers in response to a second chemoattractant, MIP-2 (macrophage inflammatory protein-2; Kobayashi, 2006). Again, no difference in behavior was detected (unpublished data). Flotillin microdomains are, therefore, neither required for neutrophils to sense different chemoattractants nor for locomotion of neutrophils on planar glass surfaces.

It is likely that there are different functional requirements for cells to migrate through resistive, three-dimensional environments than for migration on planar surfaces (Even-Ram and Yamada, 2005; Doyle et al., 2009). We assayed migration of neutrophils through Matrigel (a matrix of laminin, collagen, and other basement membrane components; Kleinman et al., 1982).

Generation of projections based on confocal Z-stacks allowed measurement of the proportion of cells migrating into a layer of Matrigel in response to chemoattractant (Fig. 5 a). We found MIP-2 gave more reproducible results in this assay than fMLP. A marked reduction in the efficiency of migration into Matrigel was observed in *flotillin 1*$^{-/-}$ neutrophils when compared with controls (Fig. 5, a and b). This suggests that the defect in neutrophil recruitment in *flotillin 1*$^{-/-}$ mice reported in Fig. 2 is, at least in part, due to a cell-intrinsic effect of the lack of flotillin microdomains specifically in neutrophils.

To look for possible defects in neutrophil polarization and uropod formation, we fixed fMLP-stimulated neutrophils from control and *flotillin 1*$^{-/-}$ mice, and stained them with antibodies against myosin IIa, α-spectrin, and against the uropod membrane marker CD44 (del Pozo et al., 1995; Fig. 5, c and d; spectrin staining shown in Fig. S3 e). The number of uropods was quantified using CD44 as a marker. *Flotillin 1*$^{-/-}$ neutrophils had a well-defined uropod half as frequently as was observed in the controls (Fig. 5 e).

To analyze whether myosin IIa activity was altered in *flotillin 1*$^{-/-}$ neutrophils we used phosphospecific antibodies to measure phosphorylation of myosin IIa RLC after stimulation with fMLP. Staining with the phosphospecific antibodies was efficiently concentrated in the uropod (Fig. 5 f). Quantification of fluorescence intensity revealed an ∼50% drop in signal in *flotillin 1*$^{-/-}$ neutrophils stimulated with fMLP for 15 min (Fig. 5 g). Reduced myosin IIa RLC phosphorylation in *flotillin 1*$^{-/-}$ neutrophils during stimulation with fMLP was confirmed by Western blotting (Fig. 5, h and i).

Conclusion

The data presented here demonstrate a requirement for flotillin microdomains during neutrophil recruitment in vivo. Our data also reveal that one of the functions of flotillin microdomains is to coordinate formation of the uropod in neutrophils; that, at least in part, this function probably involves regulation of the activity of myosin IIa; and that flotillins are required for efficient migration of neutrophils through Matrigel.

Our previous studies, and those of other laboratories, suggest that flotillins define a specific mechanism for endocytosis (Payne et al., 2007; Blanchet et al., 2008; Schneider et al., 2008; Babuke et al., 2009; Riento et al., 2009; Zhang et al., 2009). It is intriguing that immunoisolation of flotillin microdomains and analysis of associated proteins did not reveal any abundant membrane proteins. The function of flotillin-mediated endocytosis thus remains unclear. We speculate that one function may be to regulate the number and distribution of flotillin microdomains within the plasma membrane, as this could provide a way of controlling plasma membrane–cortex interactions in space and time.

---

of myosin IIa. As in panel b, but the cells were stained with phosphospecific antibodies against myosin IIa RLC. Bar, 25 μm. (d) Quantification of mean fluorescence intensity of control HeLa cells and HeLa cell lines stably overexpressing flotillin 2–GFP, labeled using immunofluorescence as in panel c. n > 20 for each sample; bars = SEM. (e) Western blots of lysates from control HeLa cells and HeLa cell lines stably overexpressing flotillin 2–GFP, probed with phosphospecific antibodies against myosin IIa RLC. (f) Western blot of lysates from HeLa cells transfected with four separate siRNAs against flotillin 1 or flotillin 2 as shown. Control cells were transfected with nonspecific siRNAs. Blots were probed with different antibodies as shown. One typical experiment is shown; the experiment was repeated four times.
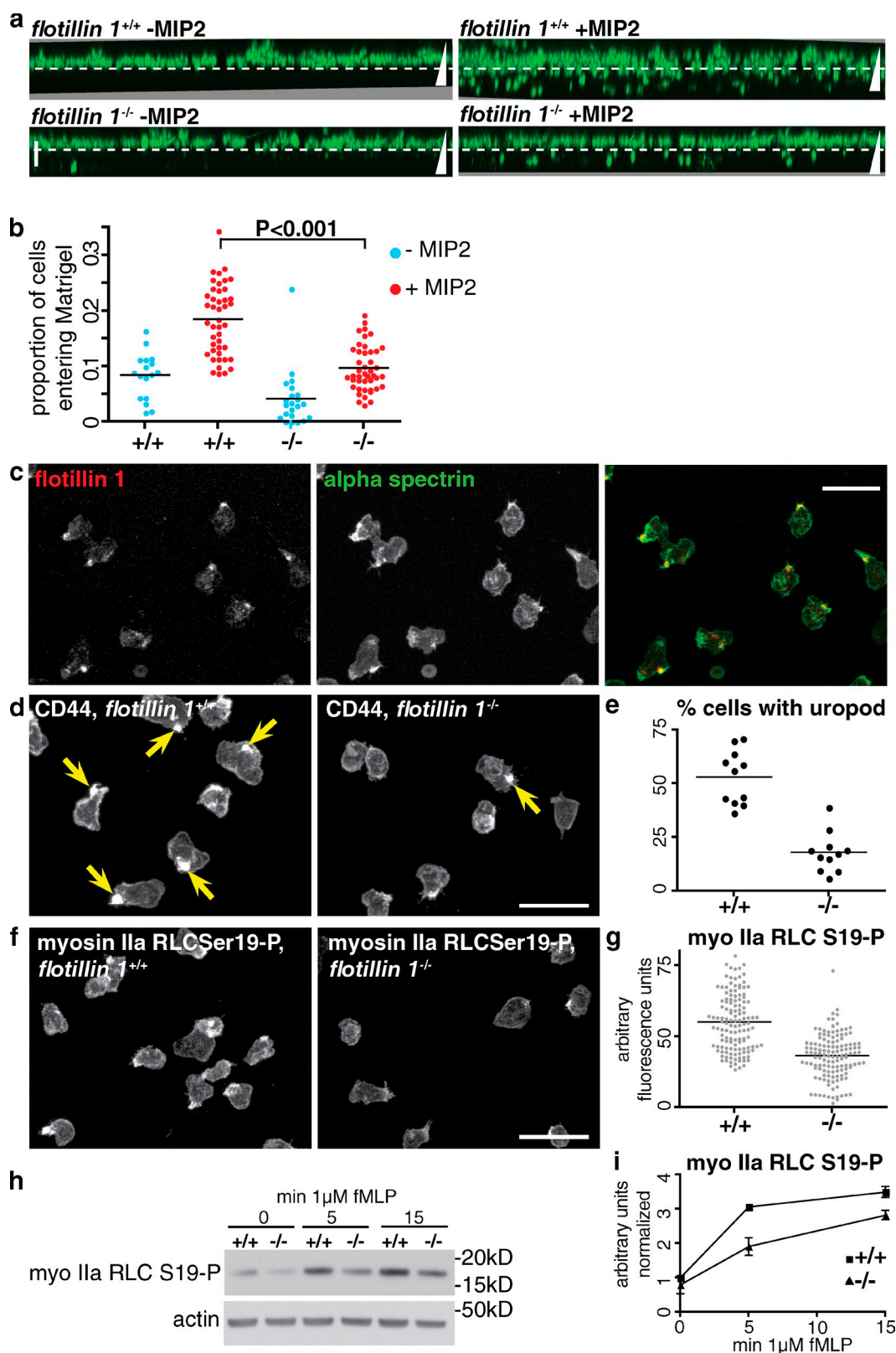
Figure 5. **Flotillin microdomains are required for uropod formation and activation of myosin IIa.** (a) Migration of control and *flotillin 1*$^{-/-}$ neutrophils into Matrigel in a gradient of MIP2. The dashed white line indicates the top of the Matrigel layer. Triangles represent the direction of the MIP2 concentration gradient; vertical bar, 50 μm. Images are maximum intensity projections derived from 20–25 confocal Z-slices. (b) Quantification of neutrophil migration into Matrigel. The proportion of cells entering the Matrigel was derived by quantifying the fluorescence above and below the dashed white line in panel a. Combined data from four separate experiments are shown. (c) Indirect immunofluorescence with antibodies against flotillin 1 and α-spectrin to show colocalization in the uropod of fMLP-stimulated neutrophils. Bar, 20 μm. (d) Comparison of uropod formation in control (+/+) and *flotillin 1*$^{-/-}$ neutrophils. Cells were fixed 15 min after stimulation with fMLP and labeled with antibodies against CD44. Arrows indicate structures defined as uropods. Bar, 20 μm.

The data clearly show functional deficits in *flotillin 1$^{-/-}$* neutrophils, but it is possible that other factors also contribute to the in vivo neutrophil recruitment phenotype—recruitment of neutrophils is a complex process involving multiple functional interactions between neutrophils, endothelial cells, and other cell types. Both our data and separate experiments on *Rac 1$^{-/-}$* neutrophils (Filippi et al., 2007) imply that the uropod itself is dispensable for neutrophil chemotaxis on planar surfaces. Our data do not, however, prove a direct link between uropod formation and the ability to migrate through resistive environments—it is possible that appropriate regulation of myosin IIa activity underlies both processes, without one being causally related to the other. Indeed, the finding that myosin II activity is needed for fibroblasts (which do not form uropods) to migrate through matrices implies that myosin II has roles in cell migration independent of uropod formation (Doyle et al., 2009).

The reduction in myosin IIa phosphorylation in both *flotillin 1$^{-/-}$* neutrophils and in flotillin siRNA-treated HeLa cells, the biochemical association between flotillin microdomains and myosin IIa, and the effect of overexpression of flotillins on myosin IIa phosphorylation all indicate that flotillin microdomains are important in regulation of myosin IIa activity. Spectrin function in uropod formation is not well characterized, but, as these proteins may restrict lateral diffusion in the plasma membrane, recruitment of spectrins could play an important role in establishment of the uropod as a distinct membrane domain (Gregorio et al., 1992; Seveau et al., 2001; Tang and Edidin, 2003; Sánchez-Madrid and Serrador, 2009). We propose that flotillin microdomains regulate uropod formation by spatially organizing the plasma membrane and the cortical cytoskeleton during neutrophil polarization, thereby allowing activation of myosin IIa and other uropod components at one specific location in the cell cortex.

Materials and methods

Mice
All animal experiments were performed in compliance with Irish Department of Health and Children regulations and approved by the Trinity College Dublin's BioResources ethical review board, or with the approval of the UK Home Office and MRC-LMB ethical review board. *Flotillin 1$^{-/-}$* C57Bl6/J mice were generated by Artemis GmbH. Gene targeting was performed in C57Bl6/J embryonic stem cells. The selectable cassette used for gene targeting (Fig. 1 a) was removed by crossing with C57Bl6/J mice that express cre recombinase (a gift from A. McKenzie, MRC-LMB). Experiments were performed both using age- and gender-matched C57Bl6/J mice as controls and comparing *flotillin 1$^{-/-}$* and *flotillin 1$^{+/+}$* littermates.

Antibodies
Mouse monoclonal antibodies against flotillin 1 (610820) and flotillin 2 (610383), rat anti-CD162 (PSGL-1; 555306), and rat anti-CD44 (560452) antibodies were from BD. Antibodies against myosin IIa (ab24762), α-spectrin (fodrin; ab11755), and pan-cadherin (ab6529) were from Abcam.

Phospho-myosin light chain 2 (Ser19; 3671) and phospho-myosin light chain 2 (Thr18/Ser19; 3674) antibodies were from Cell Signaling Technology. Anti-transferrin receptor antibody (13–6800) was from Invitrogen. Mouse anti–phospho-Erk1/2 (M8159) and polyclonal anti-actin (A2066) antibodies were from Sigma-Aldrich.

Cell culture and immunofluorescence
HeLa cells and mouse embryonic fibroblasts were cultured in DME, 10% fetal bovine serum (FBS), and penicillin/streptomycin at 37°C, 10% CO$_2$. For immunofluorescence, cells were fixed with 4% paraformaldehyde for 3–4 min followed by 6 min in −20°C methanol (MeOH). Cells were stained with primary and secondary antibodies in PBS, pH 7.4, 5% FBS, and 0.2% saponin.

Primary mouse neutrophils were stimulated with fMLP suspended in Hepes-buffered saline solution (HBSS), 15 mM Hepes, pH 7.2, and 0.05% fatty acid–free bovine serum albumin (FAF-BSA), and allowed to settle for the time indicated (typically 15 min) onto FBS-coated coverslips. They were then fixed and processed as described for HeLa cells above.

siRNA knockdown in HeLa cells
HeLa cells were transfected with 50 nM flotillin siRNAs using Oligofectamine (Invitrogen) according to the manufacturer's recommendations. The following siRNAs were used: F1.1: 5′-GCAGAGAAGUCCCAACUAA-3′; F1.2: 5′-GUGGUUAGCUACACUCUGA-3′; F2.1: 5′-UUGAGGUUGU-GCAGCGCAA-3′; F2.2: 5′-AGGCAGAGGCUGAGCGGAU-3′. All siRNAs were ordered from Thermo Fisher Scientific. Cells were lysed with RIPA buffer 72 h after transfection and lysates precipitated with MeOH/Chloroform. Equal protein amounts were subjected to Western blotting.

Image acquisition and processing
All fluorescence images were obtained using a confocal microscope (LSM 510; Carl Zeiss, Inc.), 63x 1.4 NA objective, and standard filter sets, with the exception of Fig. 4 a and Video 1. These were obtained using a total internal reflection microscope (Olympus), 100x 1.49 NA objective. Image contrast (black and white levels) was adjusted in Adobe Photoshop without gamma adjustment. Fluorescence intensities were quantified using ImageJ (NIH, Bethesda, MD).

Isolation of neutrophils
Primary mouse neutrophils were isolated from bone marrow of age- and gender-matched mice. In brief, bone marrow cells were harvested into HBSS, 15 mM Hepes, pH 7.2, and 0.05% FAF-BSA. The cell suspension (10 ml) was loaded onto a discontinuous 60/70% Percoll gradient (in HBSS; 10 ml each) and spun at 1,300 g for 30 min at 4°C. Neutrophils were collected from the 60/70% Percoll interface and washed with 50 ml HBSS, 15 mM Hepes, pH 7.2, and 0.05% FAF-BSA. Red blood cells were lysed by hypotonic shock and the final neutrophil cell pellet washed twice and resuspended in HBSS plus Ca^{2+} and Mg^{2+}, 15 mM Hepes, pH 7.2, and 0.05% FAF-BSA.

fMLP time course in neutrophils
3 × 10^6 neutrophils in HBSS plus Ca^{2+} and Mg^{2+}, 15 mM Hepes, pH 7.2, and 0.05% FAF-BSA were equilibrated to 37°C in a heat block and stimulated with 1 μM fMLP for the indicated time points. Cells were spun at 6,000 g for 1 min at 4°C and immediately lysed in RIPA buffer for 30 min on ice. Lysates were cleared of debris by centrifugation and precipitated using MeOH/CHCl$_3$.

Immunoisolation from HeLa cells
HeLa cells stably expressing flotillin 2–GFP or GFP were scraped into PBS, pelleted, and homogenized in 2 ml ice-cold HB (320 mM sucrose, 1 mM EDTA, 2 mM MgCl$_2$, 20 mM tricine, pH 7.8, plus protease Inhibitor cocktail; Roche) using a Dounce homogenizer. A post-nuclear supernatant (PNS) was generated by centrifugation of the homogenate at 1,000 g for 10 min. The PNS was buffered by the addition of one-tenth volume of 10x PBS,

(e) Quantification of the proportion of cells with a uropod, defined using CD44 as in panel d, adjacent. Data from one experiment is shown; each point represents one field of cells, n > 70 cells in each case. The experiment was repeated three times with equivalent results. (f) Comparison of phosphospecific anti-myosin IIa RLC antibody staining in control (+/+) and *flotillin 1$^{-/-}$* neutrophils. The antibody is specific to myosin IIa RLC phosphorylated at serine 19. Bar, 20 μm. (g) Quantification of mean fluorescence intensity per cell in cells labeled with the antibody specific to phosphorylated myosin IIa RLC. Data from one experiment is shown, each point represents one cell. The experiment was repeated three times with equivalent results. (h) Western blot of lysates from control (+/+) and *flotillin 1$^{-/-}$* neutrophils after stimulation with fMLP for the indicated length of time, to confirm the reduction in phosphorylation of myosin IIa RLC. (i) Densitometric quantification of Western blot of lysates from control (+/+) and *flotillin 1$^{-/-}$* neutrophils as in panel h. Signal intensities are normalized using the signal from the loading control (actin). Data from two separate experiments are shown, error bars indicate the range of signals observed.

pH 7.4, added to 60 µl anti-GFP microbeads (Miltenyi Biotec) and left on ice for 45 min with occasional mixing. The samples were applied to MACS MS separation columns (Miltenyi Biotec) followed by three washes with 3 ml PBS/0.01% Tween 20. Bulk membrane was solubilized by three consecutive washes with 70 µl ice-cold PBS/1% Triton X-100, each for 10 min (Elution 1). Detergent-resistant membranes were eluted by three washes with 70 µl PBS/1% Triton X-100/1% *n*-octyl-glucoside, each for 10 min (Elution 2). Antigen complexes were released from the beads by two washes with 70 µl 100 mM triethanolamine, pH 11.8, twice for 2 min (Elution 3). Eluate 3 was neutralized by the addition of 70 µl 1 M Tris, pH 7.4. All samples were precipitated using MeOH/CHCl₃ and separated on 4–12% NuPAGE Bis-Tris gels. For identification by mass spectrometry (MS), Coomassie-stained bands were cut out of the gel, digested with trypsin, and subjected to MS/MS.

DRM flotation gradients
Cells were pelleted by centrifugation and resuspended in 1 ml ice-cold TNE (50 mM Tris, pH 7.4, 150 mM NaCl, 5 mM EDTA, plus protease Inhibitor cocktail; Roche) followed by addition of 1 ml ice-cold 2% Triton X-100 in TNE. The lysate was mixed thoroughly and left on ice for 30 min with occasional mixing. Nuclei were pelleted at 1,000 g for 5 min. The lysate was adjusted to 40% sucrose by addition of 2 ml 80% sucrose in TNE and placed on the bottom of an ultracentrifuge tube. 6 ml 35% sucrose and 2 ml 5% sucrose (in TNE) was layered on top and the gradient spun at 35,000 rpm (SW40 rotor; Beckman Coulter) for 16 h. Twelve 1-ml fractions were collected from the bottom by tube puncture and precipitated using MeOH/CHCl₃.

Western blotting of tissue samples
Tissues from *flotillin 1⁺/⁺* and *flotillin 1⁻/⁻* littermates were homogenized in HB using a Dounce homogenizer. Equal protein amounts were solubilized by addition of RIPA buffer (25 mM Tris, pH 7.6, 150 mM NaCl, 1% NP-40, 1% sodium deoxycholate, and 0.1% SDS) and incubation on ice for 30 min. The lysates were cleared by centrifugation and the samples precipitated using MeOH/CHCl₃.

Chemotaxis assays
For chemotaxis in Dunn chambers, 50,000 bone marrow–derived neutrophils from age- and gender-matched *flotillin 1⁺/⁺* and *flotillin 1⁻/⁻* mice were allowed to adhere to glass coverslips for 10 min at room temperature in chemotaxis buffer (HBSS, 15 mM Hepes, pH 7.2, and 0.05% FAF-BSA). The Dunn chamber was assembled and an fMLP gradient of 0–100 nM was allowed to form for 15 min. Cell movement was imaged every 30 s for 30 min on an inverted microscope (Eclipse TE2000-E; Nikon) equipped with a Plan Fluor 10x 0.30 NA objective. Individual cells were tracked using the Chemotaxis tool in ImageJ.

For chemotaxis through Matrigel, purified neutrophils were labeled with Calcein AM in chemotaxis buffer for 30 min, washed twice, and resuspended in chemotaxis buffer. 2 × 10⁵ cells were added to Biocoat growth factor reduced Matrigel invasion chambers (BD), and allowed to migrate into the Matrigel in the presence or absence of 50 ng.ml⁻¹ MIP2 in the lower part of the chamber for 2 h at 37°C. Cells were then fixed in situ for 30 min in 2% PFA. Z-stacks of 10 separate fields of cells were acquired on the confocal microscope for each sample/condition. ImageJ was used to generate mean intensity projections of a view parallel to the surface of the Matrigel for each sample, and Calcein AM fluorescence intensity at the top of the Matrigel and within the Matrigel layer was measured using manually selected regions of interest.

Use of the air pouch model
Air pouches were as described previously (Smith et al., 2005). In brief, air pouches were raised by two injections, 3 d apart, of sterile air (5 ml) subcutaneously into the dorsal area of the mouse, under anesthesia. 2 d after the second injection, 1 µg of fMLP (Sigma-Aldrich) was injected into the pouch lumen. The air pouch was lavaged with PBS at a designated time point. The resultant cells were collected and quantified by flow cytometry and differential cell counting.

Intra-venous injection
Animals were anaesthetised and fMLP (300 µg/mouse) injected intravenously. After 1 h, blood was collected by cardiac puncture.

Flow cytometry
Surface marker expression was assessed by flow cytometry with data collection on a CyAn flow cytometer (Beckman Coulter). Data were analyzed using FlowJo software (Tree Star, Inc.).

Cells were stained with eBioscience mAbs; APC anti-CD11b (Mac-1 α; ICRF44), PE anti-Ly6G (RB6-8C5), and PerCP anti-F4/80 (BM8). Flow buffers used contained 2 mM EDTA to exclude doublets. Using appropriate isotype controls, gates were drawn and data were plotted on logarithmic scale density plots or dot plots.

Slide preparation and differential cell counting
Slides were prepared from the lavage fluid (50,000 cells/slide) from air pouches using a cytospin (ThermoShandon). Blood smears were prepared after cardiac puncture. All slides were stained with Wright-Giemsa (Thermo-Shandon) to depict leukocyte subsets. A total of 200 leukocytes were counted per slide.

Statistical analysis
All data are representative of mean ± SEM of between 3 and 7 replicates. Statistical analysis was performed using a Student's t test with InStat software, P-values of less than 0.05 were considered significant.

Online supplemental material
Fig. S1 shows hematological analysis of leukocyte populations in blood obtained by cardiac puncture of wild-type and *flotillin 1⁻/⁻* mice. Fig. S2 shows that stable overexpression of flotillin 2–GFP increases expression of flotillin 1. Fig. S3 shows that *Flotillin 1⁻/⁻* neutrophils chemotax on glass and detect fMLP in the same way as controls. Panel e shows comparison of α-spectrin staining in control (+/+) and *flotillin 1⁻/⁻* neutrophils. Video 1 shows co-migration of flotillin microdomains and myosin IIa. Online supplemental material is available at http://www.jcb.org/cgi/content/full/jcb.201005140/DC1.

References

Babuke, T., and R. Tikkanen. 2007. Dissecting the molecular function of reggie/flotillin proteins. *Eur. J. Cell Biol.* 86:525–532. doi:10.1016/j.ejcb.2007.03.003

Babuke, T., M. Ruonala, M. Meister, M. Amaddii, C. Genzler, A. Esposito, and R. Tikkanen. 2009. Hetero-oligomerization of reggie-1/flotillin-2 and reggie-2/flotillin-1 is required for their endocytosis. *Cell. Signal.* 21:1287–1297. doi:10.1016/j.cellsig.2009.03.012

Bickel, P.E., P.E. Scherer, J.E. Schnitzer, P. Oh, M.P. Lisanti, and H.F. Lodish. 1997. Flotillin and epidermal surface antigen define a new family of caveolae-associated integral membrane proteins. *J. Biol. Chem.* 272: 13793–13802. doi:10.1074/jbc.272.21.13793

Blanchet, M.H., J.A. Le Good, D. Mesnard, V. Oorschot, S. Baflast, G. Minchiotti, J. Klumperman, and D.B. Constam. 2008. Cripto recruits Furin and PACE4 and controls Nodal trafficking during proteolytic maturation. *EMBO J.* 27:2580–2591. doi:10.1038/emboj.2008.174

Chou, C.L., B.M. Christensen, S. Frische, H. Vorum, R.A. Desai, J.D. Hoffert, P. de Lanerolle, S. Nielsen, and M.A. Knepper. 2004. Non-muscle myosin II and myosin light chain kinase are downstream targets for vasopressin signaling in the renal collecting duct. *J. Biol. Chem.* 279:49026–49035. doi:10.1074/jbc.M408565200

Conti, M.A., and R.S. Adelstein. 2008. Nonmuscle myosin II moves in new directions. *J. Cell Sci.* 121:11–18. doi:10.1242/jcs.007112

Cooper, K.D., N. Duraiswamy, C. Hammerberg, E. Allen, C. Kimbrough-Green, W. Dillon, and D. Thomas. 1993. Neutrophils, differentiated macrophages, and monocyte/macrophage antigen presenting cells infiltrate murine epidermis after UV injury. *J. Invest. Dermatol.* 101:155–163. doi:10.1111/1523-1747.ep12363639

Coxon, P.Y., M.J. Rane, S. Uriarte, D.W. Powell, S. Singh, W. Butt, Q. Chen, and K.R. McLeish. 2003. MAPK-activated protein kinase-2 participates in p38 MAPK-dependent and ERK-dependent functions in human neutrophils. *Cell. Signal.* 15:993–1001. doi:10.1016/S0898-6568(03)00074-3

del Pozo, M.A., P. Sánchez-Mateos, M. Nieto, and F. Sánchez-Madrid. 1995. Chemokines regulate cellular polarization and adhesion receptor redistribution during lymphocyte interaction with endothelium and extracellular matrix. Involvement of cAMP signaling pathway. *J. Cell Biol.* 131:495–508. doi:10.1083/jcb.131.2.495

Doyle, A.D., F.W. Wang, K. Matsumoto, and K.M. Yamada. 2009. One-dimensional topography underlies three-dimensional fibrillar cell migration. *J. Cell Biol.* 184:481–490. doi:10.1083/jcb.200810041

Eddy, R.J., L.M. Pierini, F. Matsumura, and F.R. Maxfield. 2000. Ca2+-dependent myosin II activation is required for uropod retraction during neutrophil migration. *J. Cell Sci.* 113:1287–1298.

Even-Ram, S., and K.M. Yamada. 2005. Cell migration in 3D matrix. *Curr. Opin. Cell Biol.* 17:524–532. doi:10.1016/j.ceb.2005.08.015

Filippi, M.D., K. Szczur, C.E. Harris, and P.Y. Berclaz. 2007. Rho GTPase Rac1 is critical for neutrophil migration into the lung. *Blood.* 109:1257–1264. doi:10.1182/blood-2006-04-017731

Frick, M., N.A. Bright, K. Riento, A. Bray, C. Merrified, and B.J. Nichols. 2007. Coassembly of flotillins induces formation of membrane microdomains, membrane curvature, and vesicle budding. *Curr. Biol.* 17:1151–1156. doi:10.1016/j.cub.2007.05.078

Glebov, O.O., N.A. Bright, and B.J. Nichols. 2006. Flotillin-1 defines a clathrin-independent endocytic pathway in mammalian cells. *Nat. Cell Biol.* 8:46–54. doi:10.1038/ncb1342

Gómez-Móuton, C., J.L. Abad, E. Mira, R.A. Lacalle, E. Gallardo, S. Jiménez-Baranda, I. Illa, A. Bernad, S. Mañes, and C. Martínez-A. 2001. Segregation of leading-edge and uropod components into specific lipid rafts during T cell polarization. *Proc. Natl. Acad. Sci. USA.* 98:9642–9647. doi:10.1073/pnas.171160298

Gregorio, C.C., R.T. Kubo, R.B. Bankert, and E.A. Repasky. 1992. Translocation of spectrin and protein kinase C to a cytoplasmic aggregate upon lymphocyte activation. *Proc. Natl. Acad. Sci. USA.* 89:4947–4951. doi:10.1073/pnas.89.11.4947

Hansen, C.G., and B.J. Nichols. 2009. Molecular mechanisms of clathrin-independent endocytosis. *J. Cell Sci.* 122:1713–1721. doi:10.1242/jcs.033951

Hoehne, M., H.G. de Couet, C.A. Stuermer, and K.F. Fischbach. 2005. Loss-and gain-of-function analysis of the lipid raft proteins Reggie/Flotillin in Drosophila: they are posttranslationally regulated, and misexpression interferes with wing and eye development. *Mol. Cell. Neurosci.* 30:326–338. doi:10.1016/j.mcn.2005.07.007

Jacobelli, J., F.C. Bennett, P. Pandurangi, A.J. Tooley, and M.F. Krummel. 2009. Myosin-IIA and ICAM-1 regulate the interchange between two distinct modes of T cell migration. *J. Immunol.* 182:2041–2050. doi:10.4049/jimmunol.0803267

Kadl, A., E. Galkina, and N. Leitinger. 2009. Induction of CCR2-dependent macrophage accumulation by oxidized phospholipids in the air-pouch model of inflammation. *Arthritis Rheum.* 60:1362–1371. doi:10.1002/art.24448

Kato, N., M. Nakanishi, and N. Hirashima. 2006. Flotillin-1 regulates IgE receptor-mediated signaling in rat basophilic leukemia (RBL-2H3) cells. *J. Immunol.* 177:147–154.

Kleinman, H.K., M.L. McGarvey, L.A. Liotta, P.G. Robey, K. Tryggvason, and G.R. Martin. 1982. Isolation and characterization of type IV procollagen, laminin, and heparan sulfate proteoglycan from the EHS sarcoma. *Biochemistry.* 21:6188–6193. doi:10.1021/bi00267a025

Kobayashi, Y. 2006. Neutrophil infiltration and chemokines. *Crit. Rev. Immunol.* 26:307–316.

Lang, D.M., S. Lommel, M. Jung, R. Ankerhold, B. Petrausch, U. Laessing, M.F. Wiechers, H. Plattner, and C.A. Stuermer. 1998. Identification of reggie-1 and reggie-2 as plasmamembrane-associated proteins which cocluster with activated GPI-anchored cell adhesion molecules in non-caveolar micropatches in neurons. *J. Neurobiol.* 37:502–523. doi:10.1002/(SICI)1097-4695(199812)37:4<502::AID-NEU2>3.0.CO;2-S

Langhorst, M.F., G.P. Solis, S. Hannbeck, H. Plattner, and C.A. Stuermer. 2007. Linking membrane microdomains to the cytoskeleton: regulation of the lateral mobility of reggie-1/flotillin-2 by interaction with actin. *FEBS Lett.* 581:4697–4703. doi:10.1016/j.febslet.2007.08.074

Langhorst, M.F., A. Reuter, F.A. Jaeger, F.M. Wippich, G. Luxenhofer, H. Plattner, and C.A. Stuermer. 2008. Trafficking of the microdomain scaffolding protein reggie-1/flotillin-2. *Eur. J. Cell Biol.* 87:211–226. doi:10.1016/j.ejcb.2007.12.001

Lee, J.H., T. Katakai, T. Hara, H. Gonda, M. Sugai, and A. Shimizu. 2004. Roles of p-ERM and Rho-ROCK signaling in lymphocyte polarity and uropod formation. *J. Cell Biol.* 167:327–337. doi:10.1083/jcb.200403091

Neumann-Giesen, C., B. Falkenbach, P. Beicht, S. Claasen, G. Lüers, C.A. Stuermer, V. Herzog, and R. Tikkanen. 2004. Membrane and raft association of reggie-1/flotillin-2: role of myristoylation, palmitoylation and oligomerization and induction of filopodia by overexpression. *Biochem. J.* 378:509–518. doi:10.1042/BJ20031100

Neumann-Giesen, C., I. Fernow, M. Amaddii, and R. Tikkanen. 2007. Role of EGF-induced tyrosine phosphorylation of reggie-1/flotillin-2 in cell spreading and signaling to the actin cytoskeleton. *J. Cell Sci.* 120:395–406. doi:10.1242/jcs.03336

Payne, C.K., S.A. Jones, C. Chen, and X. Zhuang. 2007. Internalization and trafficking of cell surface proteoglycans and proteoglycan-binding ligands. *Traffic.* 8:389–401. doi:10.1111/j.1600-0854.2007.00540.x

Rajendran, L., J. Beckmann, A. Magenau, E.M. Boneberg, K. Gaus, A. Viola, B. Giebel, and H. Illges. 2009. Flotillins are involved in the polarization of primitive and mature hematopoietic cells. *PLoS One.* 4:e8290. doi:10.1371/journal.pone.0008290

Riento, K., M. Frick, I. Schafer, and B.J. Nichols. 2009. Endocytosis of flotillin-1 and flotillin-2 is regulated by Fyn kinase. *J. Cell Sci.* 122:912–918. doi:10.1242/jcs.039024

Rossy, J., D. Schlicht, B. Engelhardt, and V. Niggli. 2009. Flotillins interact with PSGL-1 in neutrophils and, upon stimulation, rapidly organize into membrane domains subsequently accumulating in the uropod. *PLoS One.* 4:e5403. doi:10.1371/journal.pone.0005403

Saito, H., Y. Minamiya, S. Saito, and J. Ogawa. 2002. Endothelial Rho and Rho kinase regulate neutrophil migration via endothelial myosin light chain phosphorylation. *J. Leukoc. Biol.* 72:829–836.

Sánchez-Madrid, F., and J.M. Serrador. 2009. Bringing up the rear: defining the roles of the uropod. *Nat. Rev. Mol. Cell Biol.* 10:353–359. doi:10.1038/nrm2680

Schneider, A., L. Rajendran, M. Honsho, M. Gralle, G. Donnert, F. Wouters, S.W. Hell, and M. Simons. 2008. Flotillin-dependent clustering of the amyloid precursor protein regulates its endocytosis and amyloidogenic processing in neurons. *J. Neurosci.* 28:2874–2882. doi:10.1523/JNEUROSCI.5345-07.2008

Seveau, S., R.J. Eddy, F.R. Maxfield, and L.M. Pierini. 2001. Cytoskeleton-dependent membrane domain segregation during neutrophil polarization. *Mol. Biol. Cell.* 12:3550–3562.

Smith, P., R.E. Fallon, N.E. Mangan, C.M. Walsh, M. Saraiva, J.R. Sayers, A.N. McKenzie, A. Alcami, and P.G. Fallon. 2005. *Schistosoma mansoni* secretes a chemokine binding protein with antiinflammatory activity. *J. Exp. Med.* 202:1319–1325. doi:10.1084/jem.20050955

Tang, Q., and M. Edidin. 2003. Lowering the barriers to random walks on the cell surface. *Biophys. J.* 84:400–407. doi:10.1016/S0006-3495(03)74860-7

Taylor, P.R., G.D. Brown, D.M. Reid, J.A. Willment, L. Martinez-Pomares, S. Gordon, and S.Y. Wong. 2002. The beta-glucan receptor, dectin-1, is predominantly expressed on the surface of cells of the monocyte/macrophage and neutrophil lineages. *J. Immunol.* 169:3876–3882.

Umemoto, S., A.R. Bengur, and J.R. Sellers. 1989. Effect of multiple phosphorylations of smooth muscle and cytoplasmic myosins on movement in an in vitro motility assay. *J. Biol. Chem.* 264:1431–1436.

Vicente-Manzanares, M., X. Ma, R.S. Adelstein, and A.R. Horwitz. 2009. Non-muscle myosin II takes centre stage in cell adhesion and migration. *Nat. Rev. Mol. Cell Biol.* 10:778–790. doi:10.1038/nrm2786

Volonte, D., F. Galbiati, S. Li, K. Nishiyama, T. Okamoto, and M.P. Lisanti. 1999. Flotillins/cavatellins are differentially expressed in cells and tissues and form a hetero-oligomeric complex with caveolins in vivo. Characterization and epitope-mapping of a novel flotillin-1 monoclonal antibody probe. *J. Biol. Chem.* 274:12702–12709. doi:10.1074/jbc.274.18.12702

Xu, J., F. Wang, A. Van Keymeulen, P. Herzmark, A. Straight, K. Kelly, Y. Takuwa, N. Sugimoto, T. Mitchison, and H.R. Bourne. 2003. Divergent signals and cytoskeletal assemblies regulate self-organizing polarity in neutrophils. *Cell.* 114:201–214. doi:10.1016/S0092-8674(03)00555-5

Zhang, D., M. Manna, T. Wohland, and R. Kraut. 2009. Alternate raft pathways cooperate to mediate slow diffusion and efficient uptake of a sphingolipid tracer to degradative and recycling compartments. *J. Cell Sci.* 122:3715–3728. doi:10.1242/jcs.051557